P H Y S I C A L   R E V I E W   L E T T E R S

# Nucleon-Nucleon Scattering from Fully Dynamical Lattice QCD

S. R. Beane,[1,2] P. F. Bedaque,[3,4] K. Orginos,[5,2] and M. J. Savage[6]

[1]*Department of Physics, University of New Hampshire, Durham, New Hampshire 03824-3568, USA*
[2]*Jefferson Laboratory, 12000 Jefferson Avenue, Newport News, Virginia 23606, USA*
[3]*Lawrence-Berkeley Laboratory, Berkeley, California 94720, USA*
[4]*Department of Physics, University of Maryland, College Park, Maryland 20742, USA*
[5]*Department of Physics, College of William and Mary, Williamsburg, Virginia 23187-8795, USA*
[6]*Department of Physics, University of Washington, Seattle, Washington 98195-1560, USA*

We present results of the first fully dynamical lattice QCD determination of nucleon-nucleon scattering lengths in the $^1S_0$ channel and $^3S_1 - {}^3D_1$ coupled channels. The calculations are performed with domain-wall valence quarks on the MILC staggered configurations with a lattice spacing of $b = 0.125$ fm in the isospin-symmetric limit, and in the absence of electromagnetic interactions.

One of the ultimate goals of nuclear physics is to compute the properties and interactions of nuclei directly from quantum chromodynamics (QCD), the underlying theory of the strong interactions. Achievement of this goal would reveal how nuclear processes depend upon the fundamental constants of nature, and would enable the computation of strong-interaction processes of importance in environments not attainable in the laboratory, such as in the interior of neutron stars. A lone, pioneering study of nucleon-nucleon (*NN*) scattering with lattice QCD was performed more than a decade ago by Fukugita *et al.* [1]. These calculations were quenched and at relatively large pion masses, $m_\pi \gtrsim 550$ MeV.

Lattice QCD is presently the only known method of calculating low-energy strong-interaction processes from QCD. However, it is unlikely that lattice QCD will ever be used to calculate the properties or interactions of nuclei beyond the lightest few. In order to compute the properties of larger nuclei, lattice QCD calculations of the lightest nuclei will be performed, and then matched to calculations of the larger nuclei using many-body techniques such as a Green's function Monte Carlo calculation, e.g., Ref. [2], or the No-Core Shell Model, e.g., Ref. [3], including up to four-body (and possibly higher) interactions consistent with chiral symmetry and power counting. These many-body methods have had great success in reproducing the properties of the light nuclei using high-precision phenomenological potentials as input and recently with the chiral potentials derived from effective field theory (EFT) expansions.

In this Letter we present results of the first fully dynamical lattice QCD calculation of the *NN* scattering lengths in both the $^1S_0$ channel and $^3S_1 - {}^3D_1$-coupled channels at pion masses of $m_\pi \sim 350$, 490, and 590 MeV in the isospin limit. Our lattice calculations are performed with domain-wall [4] valence quarks on the $20^3 \times 64$ MILC gauge-field configurations with a lattice spacing of $b \sim 0.125$ fm and a spatial extent of $L \sim 2.5$ fm. The depen-

dence of the *NN* scattering lengths upon the light-quark masses has been determined to various nontrivial orders in the EFT expansion [5], and is estimated to be valid up to $m_\pi \sim 350$ MeV. We use the results of our lattice QCD calculation at the lightest pion mass and the experimentally determined scattering lengths at the physical value of the pion mass to constrain the chiral dependence of the scattering lengths from $m_\pi \sim 350$ MeV down to the chiral limit.

The *NN* scattering lengths are determined by computing the energy shift of the lowest-lying two-nucleon state in the finite lattice volume. To extract $p \cot\delta(p)$—where $\delta(p)$ is the phase shift—the magnitude of the center-of-mass momentum, $p$, is extracted from this energy shift and inserted into Lüscher's relation [6]

$$p \cot\delta(p) = \frac{1}{\pi L}\left(\sum_{\mathbf{j}}^{|\mathbf{j}|<\Lambda} \frac{1}{|\mathbf{j}|^2 - (\frac{pL}{2\pi})^2} - 4\pi\Lambda\right), \quad (1)$$

which is valid below the inelastic threshold. The sum in Eq. (1) is over all triplets of integers $\mathbf{j}$ such that $|\mathbf{j}| < \Lambda$ and the limit $\Lambda \to \infty$ is implicit [7]. The *s*-wave scattering lengths in the *NN* systems follow from the effective range expansion (ERE)

$$p \cot\delta(p) = -\frac{1}{a} + \frac{1}{2} r p^2 + \dots, \quad (2)$$

where $a$ is the scattering length (using the nuclear physics sign convention) and $r$ is the effective range which is typically of order the range of the interaction, $\sim 1/m_\pi$.

Following the LHP collaboration (LHPC) [8], our computation is a hybrid lattice QCD calculation using domain-wall valence quarks from a smeared source on three sets of $N_f = 2 + 1$ asqtad-improved [9] MILC configurations generated with staggered sea quarks [10]. In the generation of the MILC configurations, the strange-quark mass was fixed near its physical value, $bm_s = 0.050$, (where $b$ is the lattice spacing) determined by the mass of hadrons con-

taining strange quarks. The two light quarks in the three sets of configurations are degenerate (isospin-symmetric), with masses $bm_l = 0.010$, $0.020$, and $0.030$. Some of the domain-wall valence propagators were previously generated by LHPC on each of these sets of lattices. The domain-wall height is $m = 1.7$ and the extent of the extra dimension is $L_5 = 16$. The parameters used to generate the light-quark propagators have been "tuned" so that the mass of the pion computed with the domain-wall propagators is equal (to few-percent precision) to that of the lightest staggered pion computed with the same parameters as the gauge configurations [10]. The MILC lattices were HYP-blocked [11] and Dirichlet boundary conditions were used to reduce the time extent of the MILC lattices from 64 to 32 time slices in order to save time in propagator generation. Various parts of the lattice were employed to generate multiple sets of propagators on each lattice. We analyzed one set of correlation functions on 564 lattices with $bm_l = 0.030$, three sets of correlation functions on 486 lattices with $bm_l = 0.020$, and one set of correlation functions on 658 lattices with $bm_l = 0.010$. The lattice calculations were performed with the CHROMA software suite [12] on the high-performance computing systems at the Jefferson Laboratory.

The cleanest quantity from which to extract the energy difference between the two-nucleon state(s) and the mass of two noninteracting nucleons was found to be the ratio of correlation functions

$$G^{IS}(t) = C_{NN}^{IS}(t)/[C_N(t)]^2 \to A^{IS} e^{-\Delta E^{IS} t}, \qquad (3)$$

where $I$ denotes the isospin of the $NN$ system and $S$ denotes its spin. The single-nucleon correlator is

$$C_N(t) = \sum_{\mathbf{x}} \langle N(t, \mathbf{x}) N^\dagger(0, \mathbf{0}) \rangle, \qquad (4)$$

and the two-nucleon correlator that projects onto the $s$-wave state in the continuum limit is

$$C_{NN}^{IS}(t) = X_{\alpha\beta\sigma\rho}^{ijkl} \sum_{\mathbf{x},\mathbf{y}} \langle N_i^\alpha(t, \mathbf{x}) N_j^\beta(t, \mathbf{y}) N_k^{\sigma\dagger}(0, \mathbf{0}) N_l^{\rho\dagger}(0, \mathbf{0}) \rangle, \qquad (5)$$

where $\alpha$, $\beta$, $\sigma$, and $\rho$ are isospin indices and $i$, $j$, $k$, and $l$ are Dirac indices. The tensor $X_{\alpha\beta\sigma\rho}^{ijkl}$ has elements that produce the correct spin-isospin quantum numbers of two nucleons in an $s$ wave. The summation over $\mathbf{x}$ (and $\mathbf{y}$) corresponds to summing over all the spatial lattice sites, thereby projecting onto the momentum $\mathbf{p} = \mathbf{0}$ state. The interpolating field for the proton is $p_i(t, \mathbf{x}) = \epsilon_{abc} u_i^a(t, \mathbf{x}) [u^{bT}(t, \mathbf{x}) C\gamma_5 d^c(t, \mathbf{x})]$, and similarly for the neutron. The ratio of correlation functions that we obtain in the $^1S_0$ channel and the $^3S_1 - ^3D_1$ coupled channels, at the three different pion masses, are shown in Fig. 1 and 2, respectively.

The ratio of correlation functions given in Eq. (3) becomes a simple exponential function at large times. The
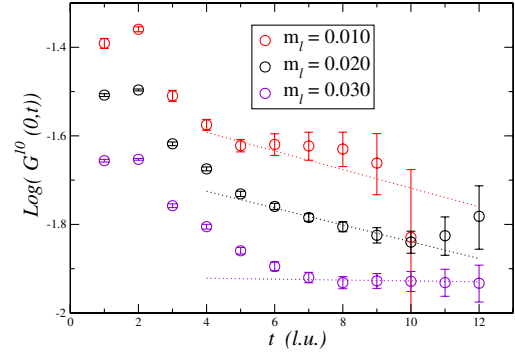


FIG. 1 (color online). The logarithm of the ratio of correlation functions in the $^1S_0$ channel ($G^{10}$) as a function of time slice. Each has been offset vertically for display purposes. The dotted lines correspond to the fit function at the central values of the fit parameters.

argument of the exponential depends upon the energy difference between the two nucleons in the finite volume and two noninteracting nucleons. Once this energy difference has been determined, it can be inserted into Eq. (1) to determine the scattering amplitude. To extract the energy differences at each of the light-quark masses, a single exponential function was fit to each ratio of correlation functions shown in Fig. 1 and 2. The errors on each time slice were determined by the jacknife procedure, as were the correlations between time slices. A correlated $\chi^2$ minimization of a two-parameter ($A$ and $\Delta E$) fit function of the form $A \exp(-\Delta E t)$ was performed over a given fitting interval. In each case, the fitting interval was established so that the extracted value of $\Delta E$ was relatively insensitive (within statistical errors) to changes of the initial and final time slice of the interval. The results of our calculations are shown in Table I. The scale is set via the quark-mass dependence of $f_\pi$, which gives $b = 0.127 \pm 0.001$ fm [13] (consistent with the Sommer scale-setting procedure used by MILC [10]). At the pion masses used in these
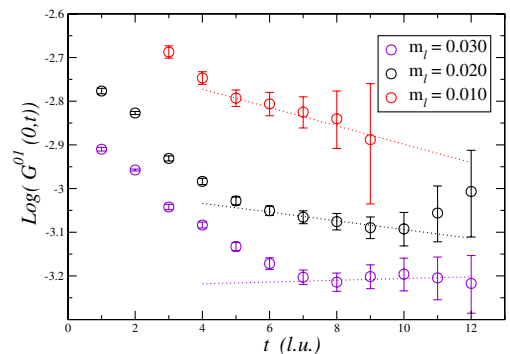


FIG. 2 (color online). The logarithm of the ratio of correlation functions in the $^3S_1 - ^3D_1$ coupled channels ($G^{01}$) as a function of time slice. Each has been offset vertically for display purposes. The dotted lines correspond to the fit function at the central values of the fit parameters.

TABLE I. Scattering lengths in the $^1S_0$ channel and in the $^3S_1 - ^3D_1$ coupled channels. The fitting ranges and fit $\chi^2$/dof are given in parentheses. Each scattering length has an additional systematic error of $\sim \pm 0.1$ fm associated with the truncation of the effective range expansion; i.e., the numbers exhibited are for $-1/p \cot\delta$ at the measured energy splitting.

| $m_\pi$ (MeV) | $a(^1S_0)$ (fm) | $a(^3S_1)$ (fm) |
|---|---|---|
| $353.7 \pm 2.1$ | $0.63 \pm 0.50$ (5–10; 0.68) | $0.63 \pm 0.74$ (5–9; 0.24) |
| $492.5 \pm 1.1$ | $0.65 \pm 0.18$ (6–9; 0.07) | $0.41 \pm 0.28$ (6–9; 0.30) |
| $593.0 \pm 1.6$ | $0.0 \pm 0.5$ (7–12; 0.30) | $-0.2 \pm 1.3$ (7–12; 0.54) |

calculations the *NN* scattering lengths are found to be of natural size in both channels, and are much smaller than the $L \sim 2.5$ fm lattice spatial extent. It is noteworthy that our scattering lengths at the heaviest pion mass are not inconsistent with the lightest-mass quenched values of Ref. [1]. However, one should keep in mind the effects of quenching on the infrared properties of the theory [14].

The lowest pion mass at which we have calculated is at the upper limit of where we expect the EFT describing *NN* interactions to be valid [15–17]. While some controversy remains regarding the details of the *NN* EFT, in our present analysis, we have constrained the chiral extrapolation using the power counting of Ref. [17] (BBSvK) [ ≡ the power counting of Ref. [16] (KSW)] and Weinberg (W) power counting [15] in the $^1S_0$ channel and BBSvK power counting in the $^3S_1 - ^3D_1$ coupled channels. The recent lattice QCD determinations of the light-quark axial-matrix element in the nucleon by LHPC [18] and its physical value are used to constrain the chiral expansion of $g_A$. Our lattice calculations of the nucleon mass and pion decay constant [13]—as well as their physical values—are used to constrain their respective chiral expansions. In addition to the quark-mass dependence these three quantities contribute to the *NN* systems, there is dependence on the quark masses at next-to-leading order (NLO) from pion exchange, and from local four-nucleon operators that involve a single insertion of the light-quark-mass matrix, described by the "$D_2$" coefficients [5]. The results of this lattice QCD calculation constrain the range of allowed values for the $D_2$'s, and consequently the scattering lengths in the region between $m_\pi \sim 350$ MeV and the chiral limit, as shown in Fig. 3 and 4. With only one lattice point at the edge of the regime of applicability of the EFT, a prediction for the scattering lengths at the physical pion mass is not possible: the experimental values of the scattering lengths are still required for an extrapolation to the chiral limit and naive dimensional analysis (NDA) is still required to select only those operator coefficients that are consistent with perturbation theory. The regions plotted in the figures correspond to values of $C_0$—the coefficient of the leading-order quark-mass independent local operator—and $D_2$ that fit the lattice datum and the physical value, and are consistent with NDA; indeed we have $D_2(\Lambda)m_\pi^2/C_0(\Lambda) \sim \pm 0.10$ in both channels (at physical $m_\pi$), at a renormalization scale $\Lambda \sim 350$ MeV. In both channels the lightest lattice datum

constrains the chiral extrapolation to two distinct bands which are sensitive to both the quark-mass dependence of $g_A$ and the sign of the $D_2$ coefficient. As the lattice point used to constrain the EFT is at the upper limits of applicability of the EFT, we expect non-negligible corrections to these regions from higher orders in the EFT expansion. It is clear from Fig. 3 and 4 that even a qualitative understanding of the chiral limit will require lattice calculations at lighter quark masses.

Without the resources to perform similar lattice QCD calculations in different volumes, we have assumed that the energy shifts at $m_\pi \sim 593$ MeV (both consistent with zero) are associated with scattering states and not bound states. Calculations in larger volumes will be done in the future to verify the expected power-law dependence upon volume that scattering states exhibit. In addition to discriminating between bound and continuum states, calculations in a larger volume would reduce the energy of the lowest-lying continuum lattice states, and thus reduce the uncertainty in the scattering length due to truncation of the ERE. Further improvement would result from measuring the energy of the first excited state on the lattice, either with a single source or by using the Lüscher-Wolff [19] method.

There are many aspects of this calculation that should be refined in the future. The statistics should be improved by at least an order of magnitude to have a precise extraction of the scattering lengths from each of these lattices. The
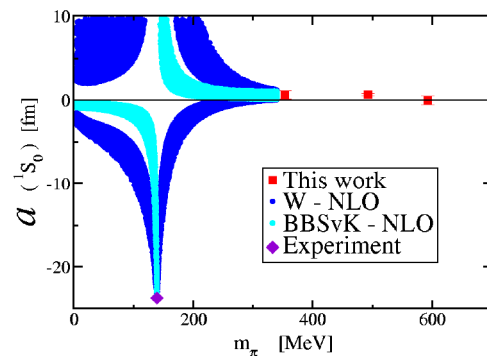


FIG. 3 (color online). Allowed regions for the scattering length in the $^1S_0$ channel as a function of the pion mass. The experimental value of the scattering length and NDA have been used to constrain the extrapolation in both BBSvK and W power countings at NLO.
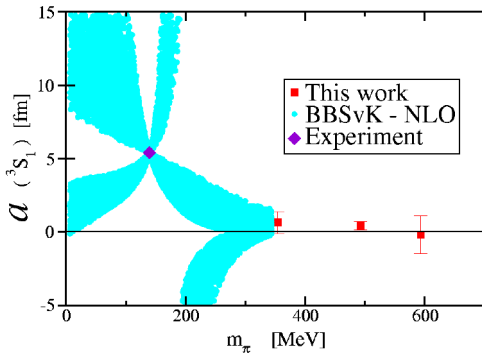
FIG. 4 (color online).   Allowed regions for the *s*-wave scattering length in the $^3S_1 - {}^3D_1$ coupled channels as a function of the pion mass. The experimental value of the scattering length and NDA have been used to constrain the extrapolation in BBSvK power counting at NLO. (W counting gives a similar result.)

lattice spacing effects in the present calculation appear at $\sim \mathcal{O}(b^2)$ [or exponentially suppressed $\mathcal{O}(b)$ effects], and are expected to be small. However, the finite lattice spacing effects should be determined by performing the same calculation on lattices with a finer lattice spacing. While it would be useful to perform this calculation with configurations generated from domain-wall quarks in the sea sector as well, the resources to do so are not currently available to us. However, a recent theoretical investigation [20] of the impact of using a mixed-action to compute $\pi\pi$ scattering [13] has shown it to be small. An analogous theoretical investigation of mixed-action EFT for *NN* scattering which would allow a continuum extrapolation remains to be carried through. In addition to more precise lattice QCD calculations through an increase in computing resources, formal developments are also required. In order to have a more precise chiral extrapolation, calculations in the various relevant EFT's must be performed beyond NLO. Furthermore, it is clear that lattice calculations at lower pion masses are essential for the extrapolation to the chiral limit, and will ultimately allow for a "prediction" of the physical scattering lengths.

    To summarize, we have performed the first QCD calculations of nucleon-nucleon scattering by using fully dynamical, mixed-action lattice QCD. This work opens up an unexplored area of nuclear physics as it is now possible to perform lattice QCD calculations of simple nuclear systems at pion masses within the range of validity of the *NN* EFT's.

[1]  M. Fukugita, Y. Kuramashi, M. Okawa, H. Mino, and A. Ukawa, Phys. Rev. D **52**, 3003 (1995).
[2]  S. C. Pieper, R. B. Wiringa, and J. Carlson, Phys. Rev. C **70**, 054325 (2004).
[3]  C. Forssen, P. Navratil, W. E. Ormand, and E. Caurier, Phys. Rev. C **71**, 044312 (2005).
[4]  D. B. Kaplan, Phys. Lett. B **288**, 342 (1992); Y. Shamir, Nucl. Phys. **B406**, 90 (1993).
[5]  S. R. Beane and M. J. Savage, Nucl. Phys. **A713**, 148 (2003); Nucl. Phys. **A717**, 91 (2003); E. Epelbaum, U. G. Meissner, and W. Gloeckle, Nucl. Phys. **A714**, 535 (2003).
[6]  M. Lüscher, Nucl. Phys. **B354**, 531 (1991).
[7]  S. R. Beane, P. F. Bedaque, A. Parreño, and M. J. Savage, Phys. Lett. B **585**, 106 (2004); Nucl. Phys. **A747**, 55 (2005).
[8]  R. G. Edwards *et al.* (LHPC Collaboration), Proc. Sci LAT2005 (2005), 056; D. B. Renner *et al.* (LHP Collaboration), Nucl. Phys. B, Proc. Suppl. **140**, 255 (2005).
[9]  K. Orginos, D. Toussaint, and R. L. Sugar (MILC Collaboration), Phys. Rev. D **60**, 054503 (1999); K. Orginos and D. Toussaint (MILC Collaboration), Phys. Rev. D **59**, 014501 (1999).
[10]  C. W. Bernard *et al.*, Phys. Rev. D **64**, 054506 (2001).
[11]  A. Hasenfratz and F. Knechtli, Phys. Rev. D **64**, 034504 (2001).
[12]  R. G. Edwards and B. Joo (SciDAC Collaboration), Nucl. Phys. B, Proc. Suppl. **140**, 832 (2005); C. McClendon, Jlab Report No. JLAB-THY-01-29, 2001.
[13]  S. R. Beane, P. F. Bedaque, K. Orginos, and M. J. Savage (NPLQCD Collaboration), Phys. Rev. D **73**, 054503 (2006).
[14]  S. R. Beane, and M. J. Savage, Phys. Lett. B **535**, 177 (2002).
[15]  S. Weinberg, Phys. Lett. B **251**, 288 (1990); Nucl. Phys. **B363**, 3 (1991); C. Ordoñez, L. Ray, and U. van Kolck, Phys. Rev. C **53**, 2086 (1996).
[16]  D. B. Kaplan, M. J. Savage, and M. B. Wise, Nucl. Phys. **B534**, 329 (1998); Phys. Lett. B **424**, 390 (1998).
[17]  S. R. Beane, P. F. Bedaque, M. J. Savage, and U. van Kolck, Nucl. Phys. **A700**, 377 (2002).
[18]  R. G. Edwards *et al.* (LHPC Collaboration), Phys. Rev. Lett. **96**, 052001 (2006).
[19]  M. Lüscher and U. Wolff, Nucl. Phys. **B339**, 222 (1990).
[20]  J. W. Chen, D. O'Connell, R. S. Van de Water, and A. Walker-Loud, Phys. Rev. D **73**, 074510 (2006).